

## Spin density of ordered FeCo: A failure of the local-spin-density approximation

E. Di Fabrizio

*Dipartimento di Fisica dell'Università di Roma "La Sapienza," Roma, Italy*

G. Mazzone

*Comitato Nazionale per la Ricerca e per lo Sviluppo dell'Energia Nucleare e delle Energie Alternative,  
Dipartimento Tecnologie Intersettoriali di Base, Centro Ricerche Energia Casaccia, Roma, Italy*

C. Petrillo and F. Sacchetti

*Istituto di Struttura della Materia del Consiglio Nazionale delle Ricerche, Via Enrico Fermi 38,  
00044 Frascati, Roma, Italy*

(Received 1 July 1988; revised manuscript received 11 July 1989)

The magnetic structure factor of an equiatomic ordered FeCo compound has been determined by measuring the coherent scattering of a polarized neutron beam from a single-crystal sample. Fourier inversion of the experimental data has allowed us to derive the magnetic moments and the spin-density symmetry at the Fe and Co sites. Considering that both  $3d$  up-spin bands are entirely full it has also been possible to derive the symmetry and the distribution of the charge density. A comparison with available state-of-the-art theoretical calculations has evidenced significant and systematic inadequacies of the local-spin-density approximation.

### I. INTRODUCTION

Despite the impressive success of the local-spin-density approximation (LSDA) in describing the ground-state properties of metals,<sup>1,2</sup> failures of the LSDA have been reported in the case of iron relative to the cohesive energy, the equilibrium crystal structure, and the equilibrium lattice parameter.<sup>3,4</sup> These discrepancies have been attributed to an inherent property of the LSDA, that is the strictly local nature of the approximation, even if numerical inaccuracies may also play a role in other less sophisticated calculations.

In addition to the quantities discussed above, the other straightforward observables derivable from LSDA are charge and spin densities (not the momentum density).<sup>5</sup> Unfortunately, the charge density contains an important contribution from core electrons so that the accuracy of the x-ray diffraction experiments has to be significantly better than 1% to be really useful for comparison purposes. In any case, some relevant information can also be derived at the present level of accuracy, particularly for what concerns the symmetry of the charge density. Contrary to the charge density, the spin density contains contributions of outer electrons only, therefore allowing us to identify failures of the theoretical calculations at the level of accuracy of current neutron scattering experiments.

In the following we report measurements of the spin density in ordered equiatomic FeCo, which appears particularly suitable to test an available state-of-the-art LSDA calculation.<sup>6,7</sup> Actually, since FeCo crystallizes in the CsCl structure,<sup>8</sup> each atom occupies a site having full cubic symmetry, and the charge and spin densities can be correctly analyzed in terms of cubic harmonics. Moreover, existing calculations show a remarkable similarity of the electronic structure of pure bcc Co and of Co in

the FeCo compound so that the experimental spin density at the Co site may be taken as reasonably representative of a hypothetical bcc Co.

Finally, we observe that the data on FeCo together with other experimental results can be used for an analysis of systematic trends present in the charge density of  $3d$  metals as a function of the number of outer electrons and of the crystal structure. In fact, the high magnetic moment of FeCo suggests that the up-spin bands are almost completely full, as evidenced also by the theoretical calculations. This property, which allows us to deduce from the spin density the symmetry and the distribution of the charge density, is very rare in bcc  $3d$  metals and alloys as a result of a number of factors, among which are probably prevalent the stability of bcc systems around the center of the  $3d$  series and the existence of a well-developed minimum in the typical bcc density-of-states curve.

### II. EXPERIMENT AND DATA REDUCTION

The experiment was performed on the polarized neutron diffractometer installed at the 1-MW Training, Research, and Isotope Production Reactor of the Centro Ricerche Energetiche Cassaccia (Rome). A standard experimental arrangement with a vertical field of 0.7 T was employed. The sample was a vertical disk of 8 mm diameter and 2.3 mm thick, with face parallel to the (110) plane. The crystal composition was determined using x-ray emission on the same sample employed in the neutron scattering experiment. The alloy was found to be equiatomic within 1%. The flipping ratios of the first 24 reflections were determined at room temperature using a wavelength  $\lambda=0.89$  Å. Standard corrections for incomplete polarization of the incoming beam, flipping

efficiency, and half-wavelength contamination were applied. To determine the amount of extinction and to measure the long-range order parameter  $S$ , the integrated intensities of (100), (110), (200), (211), and (300) were measured at  $\lambda=0.89$  and  $1.26$  Å. The flipping ratios of the first three fundamental reflections were measured averaging along the rocking curve at both wavelengths. From a linear extrapolation to zero wavelength it was observed that the extinction correction to the ratio of magnetic to nuclear scattering amplitudes was less than 11% in the case of the (110) reflection at  $\lambda=0.89$  Å. We have to observe that the extinction correction derived from the flipping ratios is the same as that we can derive from the ratios of the integrated intensities of the first three fundamental reflections as a function of wavelength, assuming secondary extinction only. As a further check we measured also the flipping ratio of the first three fundamental reflections at  $\lambda=0.89$  Å along the rocking curve. A small decrease of the observed flipping ratio is observed at the center of the rocking curve, though such a decrease [17% on the magnetic to nuclear scattering amplitude ratio of the (110) reflection] is compatible with the estimate we obtain assuming the presence of secondary extinction only.

Comparing the intensities of superlattice reflections with those of fundamental reflections the degree of order was measured to be 1.00(1). Within experimental error the same result was obtained at both wavelengths from both superlattice reflections.

The magnetization of the FeCo sample was determined

by comparison with an iron sample having the same shape and using a ballistic magnetometer. The result was  $\mu=4.814\mu_B/\text{cell}$ , in agreement with the result of Ref. 9.

Because of the shape and of the high magnetization of the present sample, the neutron-scattering data were affected by an appreciable decrease due to the demagnetizing field. Therefore, the flipping ratios of the first three fundamental reflections at  $\lambda=0.89$  Å were measured as a function of the magnetizing field. It was observed that the field could be made high enough to reach saturation of the sample and that no depolarization of the neutron beam could be detected. Therefore, all the data were corrected for a radial demagnetizing factor,<sup>10</sup> whose average value is  $N=1.140$ , calculated according to Ref. 11 and taking into account the shape of present sample. The corrected data have been used to derive the magnetic structure factors using the nuclear scattering amplitudes of 9.54 fm for Fe and 2.53 fm for Co. The measured magnetic structure factors are reported in Table I and the quoted errors take into account both the statistical error and the uncertainty of the corrections.

### III. DISCUSSION

In addition to a comparison of present results with other measurements of the magnetic form factor of Fe and Co, an analysis of the experimental structure factors in terms of spin-density symmetry allows a comparison between experimental and calculated populations of the  $E_g$

TABLE I. Magnetic structure factors for fundamental and superlattice reflections.  $\chi^2=37.1$ .

$h k l$	$\sin(\vartheta)/\lambda$	$F_m$ ( $\mu_B/\text{cell}$ )	$F_m$ (fit)
0 0 0	0	4.814±0.020	4.812
1 1 0	0.247	3.111±0.076	3.118
2 0 0	0.349	2.038±0.052	2.076
2 1 1	0.428	1.365±0.041	1.359
2 2 0	0.494	0.860±0.024	0.910
3 1 0	0.552	0.748±0.023	0.715
2 2 2	0.605	0.399±0.016	0.378
3 2 1	0.653	0.277±0.016	0.283
4 0 0	0.699	0.343±0.016	0.342
3 3 0	0.741	0.142±0.016	0.097
4 1 1	0.741	0.211±0.016	0.197
4 2 0	0.781	0.113±0.016	0.100
3 3 2	0.819	-0.013±0.017	-0.045
4 2 2	0.856	-0.013±0.017	-0.026
4 3 1	0.891	-0.073±0.018	-0.041
5 1 0	0.891	0.118±0.016	0.097
1 0 0	0.175	0.873±0.029	0.880
1 1 1	0.303	0.447±0.013	0.445
2 1 0	0.391	0.241±0.009	0.240
3 0 0	0.524	0.138±0.009	0.128
2 2 1	0.524	0.016±0.010	0.031
3 1 1	0.580	0.034±0.009	0.039
3 2 0	0.630	0.037±0.009	0.028
3 2 2	0.721	0.018±0.010	0.036
4 1 0	0.721	-0.053±0.010	-0.067

and  $T_{2g}$  subbands. To this purpose we have calculated the magnetic moments inside the bcc Wigner-Seitz (WS) cell of Fe and Co assuming equal volumes for the two atoms. Notice that while for elemental metal this approach is unambiguous as there exists a well-defined WS cell across which the Bloch boundary conditions must be satisfied, in the case of binary alloys or compounds the choice of the unit cell about each type of atom is not obvious, so the partitioning of the magnetic moment is to some extent arbitrary.

The starting point of the calculation is the magnetization density  $\rho_m(\mathbf{r})$  which is related to the magnetic structure factors  $F_m(\mathbf{G})$  through the usual Fourier expansion:

$$\rho_m(\mathbf{r}) = \frac{1}{\Omega_0} \sum_{\mathbf{G}} F_m(\mathbf{G}) \exp(i\mathbf{G}\cdot\mathbf{r}), \quad (1)$$

where  $\Omega_0$  is the cell volume,  $\mathbf{G}$  is a reciprocal-lattice vector ( $hkl$ ), and the sum runs over all  $hkl$ 's. Then, local magnetic moments and spherical form factors are defined by<sup>12,13</sup>

$$\mu_l = \frac{1}{\Omega_0} \sum_{\mathbf{G}} F_m(\mathbf{G}) \int_{\text{WS}(l)} \exp(i\mathbf{G}\cdot\mathbf{r}) d\mathbf{r}, \quad (2a)$$

$$f_l(Q) = \frac{1}{\Omega_0 \mu_l} \sum_{\mathbf{G}} F_m(\mathbf{G}) \int_{\text{WS}(l)} \frac{\sin(Qr)}{Qr} \exp(i\mathbf{G}\cdot\mathbf{r}) d\mathbf{r}, \quad (2b)$$

where the index  $l$  refers to the  $l$ th site of the crystal unit cell. The convergence of the sum of Eq. (2b) has been found to be good and to improve, as expected, with decreasing  $Q$ .

The integrals over the WS cell have been performed according to Ref. 13. As far as Eq. (2a) is concerned, we wish to note that because of symmetry constraints the fundamental reflections apart from  $G=0$  do not contribute to the local magnetic moments, or, in other words, the superlattice reflections only contribute to the difference between Fe and Co magnetic moments, while the bulk magnetization ( $G=0$  reflection) gives the sum of the two magnetic moments. This fact is very important because the extinction, which is the most serious systematic error present in structure-factor measurements, is much smaller for superlattice reflections. For this reason we consider the magnetic moments we have derived to be essentially free from any systematic error. Using the results of present calculation we have obtained the magnetic moments reported in Table II. Inspection of Table II shows that in ordered FeCo the iron magnetic moment is considerably higher than that of pure iron, while the Co magnetic moment is very similar to that found in the hexagonal phase. This behavior correlates with the fact that while the up-spin band of Co is full in both environments, the number of up-spin electrons of Fe depends on the environment. Therefore the most important result we have derived from present data is the fact that up-spin band of Fe is essentially full in the FeCo compound.

A comparison of present magnetic moments with those derived by Collins and Forsyth<sup>14</sup> from diffuse-scattering measurements is possible if one bears in mind that since the purely magnetic scattering in ferromagnetic alloys is

TABLE II. Magnetic moments of Fe and Co as deduced by Wigner-Seitz integration (see text) and from the fit described in Eq. (3) together with corresponding aspherical magnetic moments. Spin magnetic moments are reported as obtained using the  $g$  values given in the text.  $p_m$  is spin  $E_g$  population.

	Fe	Co
$\mu$ (WS)	3.053	1.761
$\mu^{\text{sph } a}$	$3.047 \pm 0.013$	$1.765 \pm 0.010$
$\mu^a$	$0.281 \pm 0.063$	$1.194 \pm 0.065$
$\mu^{\text{spin}}$	$2.921 \pm 0.018$	$1.623 \pm 0.015$
$p_m$	$0.438 \pm 0.008$	$0.694 \pm 0.016$
$p_m^b$	$0.528 \pm 0.006$	

<sup>a</sup>See Equation (3).

<sup>b</sup>Reference 20.

directly related to magnetic-moment correlations on different sites,<sup>12</sup> a diffuse-scattering experiment using unpolarized neutrons can be easily interpreted only if the magnetic moments are assumed to be independent of local environment. Moreover, while present data refer to an ordered compound, the diffuse-scattering measurements have been performed on an almost random alloy. Notwithstanding these differences, the data of Ref. 14 are in reasonable agreement with our data, thus indicating that the magnetic fluctuations in the alloy Fe<sub>50</sub>Co<sub>50</sub> are rather small and that the influence of the degree of order on the magnetic moments is relatively small. This conclusion is in agreement with lattice-parameter and bulk-magnetization measurements<sup>9</sup> which indicate that the atomic volume and the magnetic moment do not depend appreciably on the degree of order.

The spherical form factors of Fe and Co obtained from Eqs. (2a) and (2b) are shown in Figs. 1 and 2 where they are compared with other experimental results for the pure elements. In the case of bcc Fe we have drawn a spherical form factor obtained from the experiment of Shull and Yamada<sup>15</sup> with an integration in the WS cell<sup>16</sup> analogous to that used for FeCo, while for hcp Co we have plotted the experimental results of Moon.<sup>17</sup> Notice

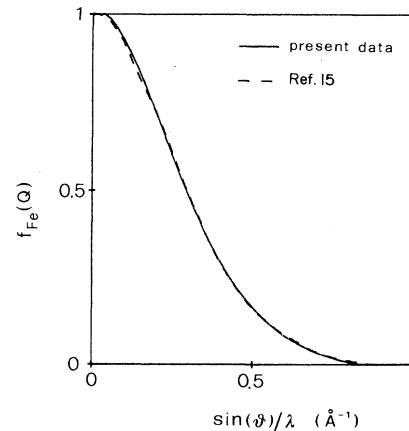


FIG. 1. Spherical form factor at the Fe site as deduced by present experimental results and compared with that of pure bcc Fe (see text).

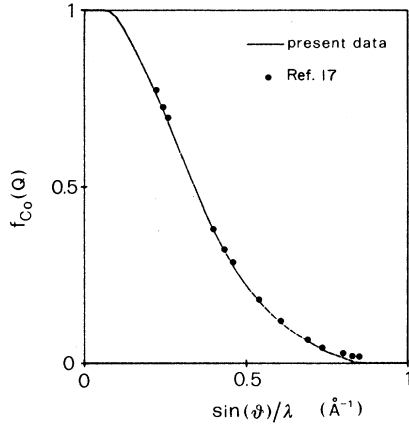


FIG. 2. Spherical form factor at the Co site as deduced by present experimental results and compared with experimental results of Ref. 17 for hcp Co.

that although the values for hcp Co are relative to the total form factor, their smooth decrease and the quantitative analysis performed in Ref. 17 indicate that the magnetic-moment distribution in hcp Co is almost spherical. Looking at Figs. 1 and 2 we see that the spherical form factors closely resembles those of pure elements.

In order to analyze the asphericity of the magnetic-moment density we have expanded the magnetic-moment density in cubic harmonics,<sup>16</sup> assuming a negligible orbital contribution to the aspherical form factor. One has

$$F_m(\mathbf{G}) = [\mu_{\text{Fe}}^{\text{sph}} f_{\text{Fe}}(\mathbf{G}) + \mu_{\text{Fe}}^a f_{\text{Fe}}^a(\mathbf{G}) + \mu_{\text{Co}}^{\text{sph}} f_{\text{Co}}(\mathbf{G}) + \mu_{\text{Co}}^a f_{\text{Co}}^a(\mathbf{G})] \exp(i\mathbf{G} \cdot \mathbf{R}_{\text{Co}}), \quad (3)$$

where  $f_{\text{Fe}}(\mathbf{G})$  and  $f_{\text{Co}}(\mathbf{G})$  are the spherical form factors, and  $f_{\text{Fe}}^a(\mathbf{G})$  and  $f_{\text{Co}}^a(\mathbf{G})$  are the aspherical form factors which we have chosen to identify with the free-atom values of  $\langle j_4 \rangle$ , as calculated by Watson and Freeman,<sup>18</sup> times the appropriate angular dependence.<sup>16</sup> This choice, although arbitrary, is nevertheless sensible since the aspherical contribution to  $F_m(\mathbf{Q})$  amounts to about 10% of  $F_m(0)$ , so that the error introduced using free-atom values of  $\langle j_4 \rangle$  is smaller than the average experimental error. In Eq. (3) the Fe atom has been placed at the origin of the unit cell, while  $\mathbf{R}_{\text{Co}}$  is the position of Co.  $\mu_{\text{Fe}}^a$  and  $\mu_{\text{Co}}^a$  are the aspherical magnetic moments which are simply related to the magnetic moments of the  $E_g$  component of the spin density:

$$\mu_{\text{Fe}}^a = \frac{5}{2} \mu_{\text{Fe}}^{E_g} - \mu_{\text{Fe}}^{\text{spin}}, \quad \mu_{\text{Co}}^a = \frac{5}{2} \mu_{\text{Co}}^{E_g} - \mu_{\text{Co}}^{\text{spin}}, \quad (4)$$

where  $\mu_{\text{Fe}}^{\text{spin}}$  and  $\mu_{\text{Co}}^{\text{spin}}$  are the spin magnetic moments of Fe and Co. These spin moments can be deduced from the corresponding spherical moments of Fe and Co using the experimental results of Ref. 19 for the gyromagnetic ratios  $g_{\text{Fe}}$  and  $g_{\text{Co}}$ . Assuming composition-independent values one has  $g_{\text{Fe}} = 2.09 \pm 0.01$  and  $g_{\text{Co}} = 2.17 \pm 0.01$ . The aspherical components of the spin magnetic moments have been obtained from a fit of Eq. (3) to the experimental magnetic structure factor leaving as free parameters all the magnetic moments. This procedure

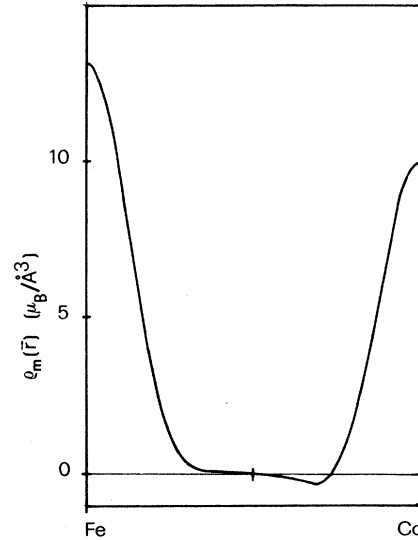


FIG. 3. Magnetic-moment density along the [111] direction.

avoids systematic errors due to the possible lack of accuracy of the flipping ratios of inner reflections which, in any case, have a little influence on the aspherical components. The results obtained with the use of Eqs. (3) and (4) are reported in Table II. One observes that the magnetic moments obtained from the fit agree quite well with those derived from the integration in the WS cell and that although the  $E_g$  population is higher than 40% for both Fe and Co the result for the iron site is considerably different from that measured in the pure metal.<sup>20</sup>

Considering that the 3d up-spin bands of Fe and Co are essentially full, present results of the spin density allow us to determine the distribution and the symmetry of the charge density if the total number of electrons on each site is known. As discussed above, in the present case the Bloch conditions do not need to be satisfied at the boundary of the WS cells with the consequence that these cells are not constrained to be electrically neutral. In order to detect a possible consequence of this effect, whose existence has been qualitatively predicted by the band calculations for FeCo, we have plotted in Fig. 3 the magnetic-moment density along the [111] direction. Although the behavior of the charge density cannot be univocally inferred from that of the spin density, we believe that the considerable asymmetry at the WS cell boundary shown by Fig. 3 is a strong indication of the lack of neutrality of the WS cells in the FeCo compound. As far as we know this is the first direct experimental indication of the existence of this effect in metallic systems. As a consequence of this circumstance the partial charges in the two sites can be deduced only under some additional hypothesis about the non- $d$ -electrons which are not constrained to have the up-spin band entirely full. The simplest and also more likely hypothesis is that in view of their essentially delocalized character the number of non- $d$ -electrons is site independent. The partial charges so deduced are listed in Table III together with the theoretical estimates of Ref. 7. We observe two main differences between the theoretical and the experimental

TABLE III. Electron distribution in the different subbands at the Fe and Co sites as deduced from both theory and experiment (see text).  $p_m$  and  $p_c$  are, respectively, spin and charge  $E_g$  populations. The theoretical populations refer to the  $d$  electrons within the atomic spheres.

	$n_{\uparrow}$	$n_{\downarrow}$	$n_{\uparrow}^d$	$n_{\downarrow}^d$	$n_{\uparrow}^{s+p}$	$n_{\downarrow}^{s+p}$	$n_{\downarrow E_g}$	$n_{\downarrow T_{2g}}$	$p_m$	$p_c$
Fe (present data)	5.386	2.465	5.000	2.079	0.386	0.386	0.721	1.358	0.438	0.384
Co (present data)	5.386	3.763	5.000	3.377	0.386	0.386	0.874	2.503	0.694	0.343
Fe (theory) <sup>a</sup>	5.31	2.59	4.61	1.86	0.67	0.71			0.432	0.382
Co (theory) <sup>a</sup>	5.40	3.71	4.67	2.94	0.70	0.74			0.565	0.361

<sup>a</sup>Reference 7.

charge distribution. The first is relative to the absolute number of electron in each subband and could be a consequence of our assumption that the up-spin  $d$ -band is full in this compound both at the Fe and Co sites. However, in this hypothesis the number of non- $d$ -electrons at each site (0.77) compares well with that of the pure metals while the band-calculated values of 1.38 at the Fe site and 1.44 at the Co site are puzzlingly high.

The second difference is relative to the spin-density asphericity at the Co site, and it is entirely contained in the experiment. As observed in other comparisons between experimental and theoretical spin densities, the qualitative trend is correctly described by the theory but the calculated asphericity is substantially smaller than in the experiment.

As already mentioned, the data obtained for the Co site can give some insight into a hypothetical bcc Co which, although not stable in bulk form at atmospheric pressure, has been the object of a theoretical calculation<sup>21</sup> at a lattice spacing much smaller than that of FeCo.

Strictly speaking, because of the orbital contribution to the magnetization density, a direct comparison of the calculated and the experimental magnetic form factor of bcc Co is not possible. However, in this case the orbital contribution is rather small and it can be calculated approximately using free-atom values of the radial charge density. Shown in Fig. 4 are the experimental and the band-theoretical<sup>21</sup> total magnetic form factors obtained from

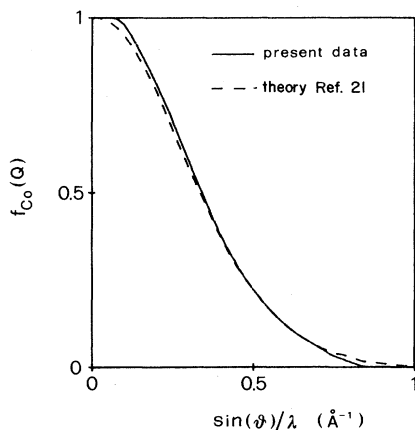


FIG. 4. Spherical form factor at the Co site as deduced by present experimental results and compared with that obtained by the theoretical calculation of Ref. 21 for pure bcc Co.

an integration in the WS cell. From the difference between the two curves one deduces that the overall shape of the theoretical spin density in bcc Co is not very different from that measured in the FeCo at the Co site. Nevertheless, in our opinion this comparison cannot be considered as a definite test of the theory because the calculation has been performed at a lattice parameter of 2.77 Å, while the experimental value for FeCo is 2.863 Å.

#### IV. CONCLUDING REMARKS

The results of this experiment confirm the difficulties of band theory to describe quantitatively electron distributions in transition metals.

A clear indication of this fact is shown in Fig. 5 where we have plotted the  $T_{2g}$  percentage of the charge density as a function of the number of outer electrons for both bcc and fcc structures. With the exception of Ni and FeCo, these values have been obtained from x-ray scattering experiments.<sup>22-25</sup> This plot is particularly meaningful since the charge-density asphericity reflects globally the distribution of  $E_g$  and  $T_{2g}$  states. Looking at Fig. 5 one has that all bcc systems show a considerable preference for  $T_{2g}$  symmetry. Moreover, the  $T_{2g}$  percentage seems to vary smoothly with the number of outer electrons, particularly if one considers that the onset of ferromagnetism disrupts the monotonic filling of the  $3d$  band. The only exception is relative to iron in the FeCo

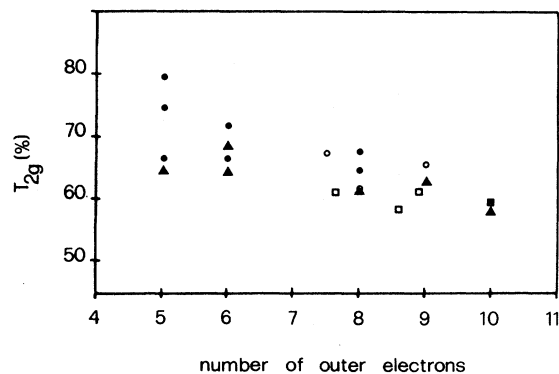


FIG. 5. Charge asphericity in the  $3d$  series. ●, experiment on pure bcc metals (Refs. 22 and 25); ○, experiment on bcc alloys (Ref. 23 and present paper); ■, experiment on pure fcc metals (Ref. 22); □, experiment on fcc alloys (Ref. 24); ▲, theory (Refs. 7 and 26-30).

compound, which is characterized by an extremely high value of the magnetic moment. On the other hand, fcc systems have an almost spherical charge density. In this connection one notices that when the number of outer electrons is in the range 7.65–9, experimental data are available on both types of structure, so that the correlation of charge asphericity and crystal structure is reasonably well established. Reported in Fig. 5 are also the theoretical LSDA estimates<sup>7,26–30</sup> when available. The calculated asphericities fail to reproduce the difference between the two structures; in particular the bcc systems appear to have a charge density definitely more spherical than experimentally measured.

This behavior is probably a basic failure of the theoretical approach, since the state-of-the-art calculations represent a virtually exact solution of the Kohn-Sham

equations<sup>1</sup> within the LSDA. However, within the LSDA it is clear that both Fermi and Coulomb holes around each electron are assumed to be spherically symmetrical, thus introducing some spherical average of the exchange-correlation potential. This fact could be the origin of the failures of theory, but an improvement of the theoretical approach is not straightforward. In fact some degree of nonlocality of the potential seems essential in order to deal with nonspherical Fermi and Coulomb holes, but very little has been done in this direction.<sup>31–33</sup> Considering that the inadequacy of local descriptions of the exchange-correlation potential was also inferred by Bauer and Schneider<sup>34</sup> when interpreting, in a very accurate way, Compton-profile data, it seems that the need for a nonlocal description of the band structure of 3d metals is a quite definite conclusion.

<sup>1</sup>S. Lundqvist and N. H. March, *Theory of the Inhomogeneous Electron Gas* (Plenum, New York, 1983).

<sup>2</sup>V. L. Moruzzi, J. F. Janak, and H. R. Williams, *Calculated Electronic Properties of Metals* (Pergamon, New York, 1978).

<sup>3</sup>H. J. F. Jansen, K. B. Hathaway, and A. J. Freeman, *Phys. Rev. B* **30**, 6177 (1984).

<sup>4</sup>H. J. F. Jansen and S. S. Peng, *Phys. Rev. B* **37**, 2689 (1988).

<sup>5</sup>G. E. W. Bauer, *Phys. Rev. B* **27**, 5912 (1983).

<sup>6</sup>K. Schwartz and D. R. Salahub, *Phys. Rev. B* **25**, 3427 (1982).

<sup>7</sup>K. Schwartz, P. Mohn, P. Blaha, and J. Kubler, *J. Phys. F* **14**, 2659 (1984).

<sup>8</sup>M. Hansen, *Constitution of Binary Alloys* (McGraw-Hill, New York, 1958).

<sup>9</sup>D. I. Bardos, *J. Appl. Phys.* **40**, 1371 (1969).

<sup>10</sup>R. M. Bozorth, *Ferromagnetism* (Van Nostrand, Princeton, 1951).

<sup>11</sup>R. M. White, *Quantum Theory of Magnetism* (Springer-Verlag, New York, 1983), p. 190.

<sup>12</sup>F. Sacchetti, *J. Phys. F* **8**, 2011 (1978).

<sup>13</sup>F. Sacchetti, *J. Phys. F* **14**, 1227 (1984).

<sup>14</sup>M. F. Collins and J. B. Forsyth, *Philos. Mag.* **8**, 401 (1963).

<sup>15</sup>C. G. Shull and Y. Yamada, *J. Phys. Soc. Jpn.* **17**, Suppl. BIII, 1 (1961).

<sup>16</sup>F. Menzinger and F. Sacchetti, *Nukleonika* **24**, 737 (1979).

<sup>17</sup>R. M. Moon, *Phys. Rev.* **136**, A195 (1964).

<sup>18</sup>R. E. Watson and A. J. Freeman, *Acta Crystallogr.* **14**, 27 (1961).

<sup>19</sup>R. A. Reck and D. L. Fry, *Phys. Rev.* **184**, 492 (1969).

<sup>20</sup>G. Frollani, F. Menzinger, and F. Sacchetti, *Phys. Rev. B* **11**, 2030 (1975).

<sup>21</sup>D. Bagayoko, A. Ziegler, and J. Callaway, *Phys. Rev. B* **27**, 7046 (1983).

<sup>22</sup>M. Diana and G. Mazzone, *Phys. Rev. B* **18**, 6631 (1978), and references therein.

<sup>23</sup>R. Cannata and G. Mazzone, *Philos. Mag.* **43**, 161 (1981).

<sup>24</sup>C. Andreani, G. Mazzone, and F. Sacchetti, *J. Phys. F* **17**, 1419 (1987).

<sup>25</sup>S. Ohba, Y. Saito, and Y. Noda, *Acta Crystallogr. Sect. A* **38**, 725 (1982) and references therein.

<sup>26</sup>D. G. Laurent, C. S. Wang, and J. Callaway, *Phys. Rev. B* **17**, 455 (1978).

<sup>27</sup>D. G. Laurent, J. Callaway, J. L. Fry, and N. E. Brener, *Phys. Rev. B* **23**, 4977 (1981).

<sup>28</sup>P. E. S. Persson and L. J. Johansson, *Phys. Rev. B* **34**, 2284 (1986).

<sup>29</sup>C. S. Wang and J. Callaway, *Phys. Rev. B* **15**, 298 (1977).

<sup>30</sup>J. Callaway and C. S. Wang, *Phys. Rev. B* **16**, 2095 (1977).

<sup>31</sup>O. Gunnarsson, M. Jonson, and B. I. Lundqvist, *Phys. Rev. B* **20**, 3136 (1979).

<sup>32</sup>M. S. Hybertsen and S. G. Louie, *Phys. Rev. B* **30**, 5777 (1984).

<sup>33</sup>M. Norman and D. D. Koelling, *Phys. Rev. B* **28**, 4357 (1983).

<sup>34</sup>G. E. W. Bauer and J. R. Schneider, *Z. Phys. B* **54**, 17 (1983).